Supplementary Material Available: Table V, a listing of structure factor amplitudes (3 pages). Ordering information is given on any current masthead page.

References and Notes

(1) R. J. H. Clark, "The Chemistry of Titanium and Vanadium", Elsevier, Amsterdam, The Netherlands, 1968.
(2) K. Watenpaugh and C. N. Caughlan, *Inorg. Chem.*, **5**, 1782 (1966).
(3) H. Hoppe and W. Haase, *Acta Crystallogr., Sect. B*, **24**, 281 (1968).
(4) N. W. Alcock, M. Pierce-Butler, and G. R. Willey, *J. Chem. Soc., Chem. Commun.*, 627 (1974).
(5) N. W. Alcock, M. Pierce-Butler, and G. R. Willey, *J. Chem. Soc., Dalton Trans.*, 707 (1976).
(6) A. Felta, *Z. Chem.*, **7**, 158 (1967).
(7) D. M. Puri, K. C. Pande, and R. C. Mehrotra, *J. Less-Common Met.*, **4**, 393 (1962).
(8) D. M. Puri, K. C. Pande, and R. C. Mehrotra, *J. Less-Common Met.*, **4**, 481 (1962).
(9) D. M. Puri and K. C. Mehrotra, *J. Less-Common Met.*, **3**, 247 (1961).
(10) D. M. Puri and R. C. Mehrotra, *J. Less-Common Met.*, **3**, 253 (1961).
(11) D. W. Thompson, W. A. Sommers, and M. O. Workman, *Inorg. Chem.*, **9**, 1252 (1970).
(12) C. E. Holloway and A. E. Sentek, *Can. J. Chem.*, **49**, 519 (1971).
(13) D. W. Thompson, R. W. Rosser, and P. B. Barrett, *Inorg. Nucl. Chem. Lett.*, **7**, 931 (1971).
(14) E. C. Alyea and P. H. Merrell, *Inorg. Nucl. Chem. Lett.*, **9**, 69 (1973).
(15) N. Serpone, P. H. Bird, D. G. Bickley, and D. W. Thompson, *J. Chem. Soc., Chem. Commun.*, 217 (1972).
(16) R. C. Fay and R. N. Lowry, *Inorg. Chem.*, **6**, 1512 (1967).
(17) N. Serpone and R. C. Fay, *Inorg. Chem.*, **6**, 1835 (1967).
(18) D. W. Thompson, personal communication.
(19) Fourier and Patterson calculations were performed using FORDAP by A. Zalkin. Structure factor and least-squares calculations were computed using SFLS-5 by C. T. Prewitt and NUCLS4 by J. A. Ibers. The diagrams were plotted using ORTEP by C. K. Johnson.
(20) "International Tables for X-Ray Crystallography", Vol. 3, Kynoch Press, Birmingham, England, 1962, p 202.
(21) Supplementary material.
(22) R. N. Lowry, Ph.D. Thesis, Cornell University, Ithaca N.Y., 1969.
(23) N. Serpone, Ph.D. Thesis, Cornell University, Ithaca, N.Y., 1969.
(24) J. R. Ferraro, "Low-Frequency Vibrations of Inorganic and Coordination Compounds", Plenum Press, New York, N.Y., 1971, Chapter 6.
(25) R. S. P. Coutts and P. C. Wailes, *J. Organomet. Chem.*, **84**, 47 (1975).
(26) R. S. P. Coutts, P. C. Wailes, and R. L. Martin, *J. Organomet. Chem.*, **47**, 375 (1973).
(27) T. J. Kistenmacher and G. J. Stucky, *Inorg. Chem.*, **10**, 122 (1971).
(28) R. J. H. Clark and M. A. Coles, *J. Chem. Soc., Dalton Trans.* 2454 (1972).
(29) L. Brun, *Acta Crystallogr.*, **20**, 739 (1966).
(30) C-I. Branden and I. Lindquist, *Acta Chem. Scand.*, **14**, 726 (1960).
(31) K. Watenpaugh and C. N. Caughlan, *Inorg. Chem.*, **6**, 963 (1967).
(32) G. D. Smith, C. N. Caughlan, and J. A. Campbell, *Inorg. Chem.*, **11**, 2989 (1972).
(33) E. C. Lingafelter, *Coord. Chem. Rev.*, **1**, 151 (1966).
(34) P. H. Bird, A. R. Fraser, and C. F. Lau, *Inorg. Chem.*, **12**, 1322 (1973).
(35) R. C. Fay and N. Serpone, *J. Am. Chem. Soc.*, **90**, 5701 (1968).
(36) "Tables of Interatomic Distance and Configuration in Molecules and Ions" *Chem. Soc., Spec. Publ.*, Supplement, No. **18**, M20S (1965).
(37) Calculated from the data reported in ref 34.
(38) A. Somogyvari and N. Serpone, to be submitted for publication.
(39) R. E. Collis, *J. Chem. Soc. A*, 1895 (1969).
(40) V. Fawcett, Ph.D. Thesis, University of London, 1967.

Contribution from the Department of Chemistry,
Texas A&M University, College Station, Texas 77843

Self-Consistent Field Xα Scattered-Wave Treatment of the Electronic Structures of Octachlorodimetalate Anions of Technetium and Tungsten

F. ALBERT COTTON* and BARBARA J. KALBACHER

Received December 29, 1976　AIC60931T

The ground-state electronic structures of the anions $Tc_2Cl_8^{3-}$ and $W_2Cl_8^{4-}$ have been calculated using the SCF–Xα–SW method. The results are discussed and compared with those already published for $Mo_2Cl_8^{4-}$ and $Re_2Cl_8^{2-}$. The electronic structure predicted for $W_2Cl_8^{4-}$ is very similar to that for $Mo_2Cl_8^{4-}$ and there does not appear to be any qualitative reason that $W_2Cl_8^{4-}$ should not be capable of existence. For the $Tc_2Cl_8^{3-}$ ion the excess electron, over the quota required for the formation of the quadruple bond between the metal atoms, occupies the $\delta^*(2b_{1u})$ orbital, making the net Tc–Tc bond order here 3.5. The calculation on $Tc_2Cl_8^{3-}$ has been carried through to a prediction, via the transition-state formalism, of the optical spectrum, apparently in good accord with the limited data available. Overall trends observed when the results of calculations for $Tc_2Cl_8^{3-}$, $Mo_2Cl_8^{4-}$, $W_2Cl_8^{4-}$, and $Re_2Cl_8^{2-}$ are all compared are discussed and found to be reasonable.

The existence of quadruple bonds between atoms of transition metals has been recognized since 1964.[1,2] In general, quadruply bonded systems have been characterized by their short metal–metal bond lengths and, in the case of $M_2X_8^{n-}$ species with eight separate ligands, by their eclipsed conformation.[3] Only recently, however, have quantitative theoretical studies been undertaken on these systems. This has occurred, in part, because of the advent of a first-principles theoretical method capable of handling multi-electron systems with the expenditure of acceptable amounts of computer time.

We report here the study of two complexes by the self-consistent field Xα scattered-wave (SCF–Xα–SW) method.[4-8] Calculations on octachloroditechnetate(2.5) and the hypothetical species, octachloroditungstate(II), were undertaken. Our purpose in treating the first one was to obtain as reliable a theoretical basis as possible on which to analyze the available experimental data for $Tc_2Cl_8^{3-}$, both published[9-15] and unpublished.[16] For $W_2Cl_8^{4-}$ we were looking for indications concerning the likelihood of its existence since it has not been reported even though it is vertically homologous to $Mo_2Cl_8^{4-}$ and horizontally homologous to $Re_2Cl_8^{2-}$, both of which are quite stable and very well characterized.

We have been mindful of the interesting and useful results already obtained on the octachlorodimolybdate[17,18] and octachlorodirhenate[19] systems by others, and we shall later compare our results in detail with these others in order to see what trends and regularities there may be as a function of net charge and position in the periodic table for the four $M_2Cl_8^{n-}$ species.

Procedures

General Data. The SCF–Xα scattered-wave method as developed by Slater and Johnson[5] was used to determine the ground-state electronic structures of $Tc_2Cl_8^{3-}$ and the hypothetical species $W_2Cl_8^{4-}$. The coordinate system was in each case applied to an ion of idealized D_{4h} symmetry with the metal–metal bond along the z axis and chlorine–metal bond directions chosen to project upon the x and y axes. The calculation of the technetium system included the use of s-, p-, and d-type spherical harmonics on the central metal and s- and p-type spherical harmonics on the chlorine ligands. For the tungsten system, s-, p-, d-, and f-type spherical harmonics were used. For the extramolecular region, spherical harmonics up to $l = 5$ were used for both systems. Throughout the calculations, the stablizing influence of a surrounding crystal lattice on the anionic complexes was stimulated by adding to the potential that of a "Watson sphere" with radius equal to that of the outer sphere.[20] All calculations were carried out on a model 470V/6 Amdahl computer. Typically, one iteration on the spin-restricted $Tc_2Cl_8^{3-}$ system required 16 s of computer time. A single iteration on the spin-unrestricted system required approximately 27 s.

Calculation on $Tc_2Cl_8^{3-}$. Coordinates for $Tc_2Cl_8^{3-}$ were taken from the crystallographic data of Cotton and Shive.[15] The averaged di-

Table I. Atomic Coordinates, α Parameters, and Sphere Radii for $Tc_2Cl_8^{3-}$ (Atomic Units)

	x	y	z	α	R
Tc(1)	0.0	0.0	2.0002	0.70320	2.4847
Tc(2)	0.0	0.0	−2.0002	0.70320	2.4847
Cl(1)	−4.3189	0.0	3.1422	0.72325	2.6684
Cl(2)	0.0	−4.3189	3.1422	0.72325	2.6684
Cl(3)	0.0	4.3189	3.1422	0.72325	2.6684
Cl(4)	4.3189	0.0	3.1422	0.72325	2.6684
Cl(5)	−4.3189	0.0	−3.1422	0.72325	2.6684
Cl(6)	0.0	−4.3189	−3.1422	0.72325	2.6684
Cl(7)	0.0	4.3189	−3.1422	0.72325	2.6684
Cl(8)	4.3189	0.0	−3.1422	0.72325	2.6684
Extramolecular	0.0	0.0	0.0	0.71548	7.6543

mensions used were as follows: Tc–Tc = 2.117 Å, Tc–Cl = 2.364 Å, and the Tc′–Tc–Cl bond angle = 104.8°. Experimental bond distances were converted to bohrs using the relation 1 bohr = 0.52917 Å. The α exchange parameter for Cl was taken from the work by Schwarz[21] and the α exchange parameter for Tc was graphically extrapolated from the same data. The α parameter used for the outer-sphere and inner-sphere regions was a weighted average (based on the number of electrons) of the α parameters of Tc and Cl. The outer sphere was positioned at the center of the molecule. A "Watson sphere" of tripositive charge and with a radius equal to that of the outer sphere was used in the calculation to simulate the stabilizing influence of the surrounding crystal lattice. Overlapping-sphere radii were chosen in the manner previously employed by Norman.[22] Atomic coordinates, sphere radii, and α parameters are listed in Table I.

The molecular potential was initially constructed from a superposition of the SCF-Xα atomic potentials of Tc +0.2 and Cl −0.425. Symmetry (D_{4h}) was used to factor the secular matrix. An average of the initial and final potentials in a 9:1 ratio, respectively, for a given iteration was used as the starting potential for the next iteration. Calculations with frozen core levels were performed for the first seven iterations. The Tc, 1s, 2s, 2p, 3s, 3p, 3d, 4s, and 4p levels and Cl 1s, 2s, and 2p levels were unfrozen for the next six iterations. Convergence to within 0.1% in the one-electron eigenvalues was achieved at this point. The spin-restricted one-electron eigenvalues are given in Table II for valence levels. Spin-unrestricted calculations were carried out for the next 16 iterations. Again, agreement of the one-electron eigenvalues in consecutive iterations to within 0.1% was the criterion for convergence. These values along with the distribution of charge between the Tc and Cl outer and inner spheres are given, for the valence orbitals, in Table III. The energies of core orbitals for both spin-restricted and spin-unrestricted calculations are available as supplementary material. The total energies and charge distributions for the spin-restricted and spin-unrestricted cases are listed in Table IV.

The final ground-state potential was used to search for virtual orbitals up to −0.020 Ry. This potential was then used as a starting point to generate the electronic spectrum using the transition-state procedure.[5,7] Typically, 12 iterations were required to achieve convergence. Figure 1 shows the upper valence region, including several of the lowest unoccupied spin-orbits.

Contour plots were generated from numerical values of the wave function at 6561 grid points within the area of the plot. Contour values are given in units of (electrons/bohr^3)$^{1/2}$. Such plots for the $\sigma(4a_{1g})$, $\sigma(2a_{1g})$, $\pi(5e_u)$, $\delta(2b_{2g})$ and $\delta^*(2b_{1u})$ orbitals, all of which possess predominant metal d character, are shown in Figures 2–6.

Calculation on $W_2Cl_8^{4-}$. The atomic potentials for $W_2Cl_8^{4-}$ were generated assuming a positive charge of 0.20 on each tungsten atom and a negative charge of 0.55 on each chlorine atom. The atomic potentials thus obtained were used to generate the molecular potential assuming idealized D_{4h} symmetry as for $Tc_2Cl_8^{3-}$. Since there were no crystallographic data for any tungsten quadruply bonded system when this work was done, molecular coordinates were assumed in the following manner. The W–W bond distance was estimated as 2.20 Å, i.e., as 0.06 Å greater than the metal–metal bond distance in the analogous molybdenum system. The tungsten to chlorine bond length was estimated to be longer than the Mo–Cl distance by 0.01 Å, and the W–W–Cl bond angle was put at 105°, identical with the Mo–Mo–Cl bond angle in $Mo_2Cl_8^{4-}$. These coordinates result in a chlorine–chlorine nonbonded contact of 3.28 Å compared to the corresponding distance of 3.22 Å in $Mo_2Cl_8^{4-}$. The α value of W was obtained by a graphical estimation based on the value of α for atoms of lower atomic number and the projected change in slope of the plot of α vs. Z for large Z.[21] The α value so estimated falls slightly above the optimized α value calculated for the 5d series by Schwarz[23] and slightly below the α value obtained by Kmetko.[24] Sphere radii were derived from those necessary to incorporate 74 electrons for tungsten and 17.5 electrons for each chlorine atom based on the output of the molecular potential program. The final radii were taken as midway between the values thus obtained and the touching radius for each sphere. Atomic coordinates, α parameters, and sphere radii are listed in Table V. The core levels of both tungsten and chlorine atoms were held invariant through the first 12 iterations. The tungsten core levels were then unfrozen and convergence of the one-electron eigenvalues was achieved in 23 iterations. The core levels of chlorine were kept frozen throughout the calculation.

Table II. Ground-State Valence Energy Levels (Rydbergs) and Charge Distribution of $Tc_2Cl_8^{3-}$ for the Spin-Restricted Case[a]

Level	Energy	% 2 Tc	% 8 Cl	% OS	% IS
$5a_{2u}$	−0.018	2.2	4.2	79.8	13.7
$6e_u$	−0.026	0.0	5.6	72.7	21.5
$5a_{1g}$	−0.071	0.9	5.4	62.4	31.3
$4b_{2u}$	−0.133	60.5	28.9	5.5	5.1
$4a_{2u}$	−0.144	71.5	8.9	1.3	18.2
$4b_{1g}$	−0.168	55.6	31.6	5.6	7.2
$5e_g$	−0.182	82.3	9.7	0.2	7.8
$2b_{1u}$	−0.329	83.6	11.7	0.5	4.2
$2b_{2g}$	−0.382	72.1	15.5	1.1	11.3
$5e_u$	−0.462	45.1	41.9	1.7	11.3
$1a_{1u}$	−0.488	0	80.1	10.5	9.3
$3b_{2u}$	−0.496	0	89.5	0.4	10.1
$1a_{2g}$	−0.502	0	78.5	10.4	11.1
$4e_g$	−0.512	1.1	87.3	4.1	7.6
$3e_g$	−0.522	2.8	84.5	0.3	12.4
$4e_u$	−0.541	7.8	78.3	3.0	10.8
$3a_{2u}$	−0.549	3.8	79.8	2.3	14.1
$3b_{1g}$	−0.567	0.9	82.6	0.2	16.2
$4a_{1g}$	−0.600	31.6	56.9	1.4	10.8
$3e_u$	−0.600	3.2	80.1	2.4	14.4
$2e_g$	−0.612	10.3	77.2	0.3	12.2
$1b_{1u}$	−0.635	12.1	70.5	1.7	15.7
$3a_{1g}$	−0.640	22.2	63.2	1.6	13.0
$2a_{2u}$	−0.647	13.0	78.1	2.8	6.2
$2b_{2u}$	−0.658	32.6	64.1	3.3	0
$1b_{2g}$	−0.669	16.3	63.1	1.2	19.5
$2e_u$	−0.674	39.7	47.2	1.0	12.0
$2b_{1g}$	−0.699	34.5	60.8	2.1	2.6
$2a_{1g}$	−0.736	66.7	32.3	1.0	0
$1b_{2u}$	−1.401	2.2	94.9	1.0	1.8
$1e_g$	−1.405	1.3	94.5	0.7	3.5
$1b_{1g}$	−1.417	2.6	93.6	0.6	3.2
$1e_u$	−1.418	1.3	93.6	0.8	4.3
$1a_{2u}$	−1.429	2.0	93.2	0.8	4.0
$1a_{1g}$	−1.446	2.3	91.7	0.6	5.3

[a] The highest occupied level is the $2b_{1u}$ level. The unoccupied levels were generated using the potential output for the final converged iteration of the ground state. Values for the charge distribution are given as the percent of charge in each level divided among the metal atoms, ligand atoms, and outer-sphere (OS) and inner-sphere (IS) regions.

The eigenvalues of all one-electron valence orbitals for $W_2Cl_8^{4-}$ are listed in Table VI, along with the charge distributions. The energies of the core orbitals are available as supplementary material. The ground-state total energy and the total charge distribution are given in Table IV. The eigenvalues for the upper valence level orbitals are shown in an energy level diagram in Figure 7.

Contour plots (Figures 8–11) were generated from numerical values of the wave function at 6561 grid points within an area of 16 × 16 bohr^2. Contour values are given in units of (electrons/bohr^3)$^{1/2}$.

Discussion

Ground State of $Tc_2Cl_8^{3-}$. A point of great interest regarding the ground-state electron distribution in $Tc_2Cl_8^{3-}$ has to do with the nature of the orbital occupied by the odd or excess electron, the valence electron present in addition to those in $Mo_2Cl_8^{4-}$ and $Re_2Cl_8^{2-}$. Shortly after the existence of the discrete $Tc_2Cl_8^{3-}$ ion was unequivocally demonstrated and its D_{4h}

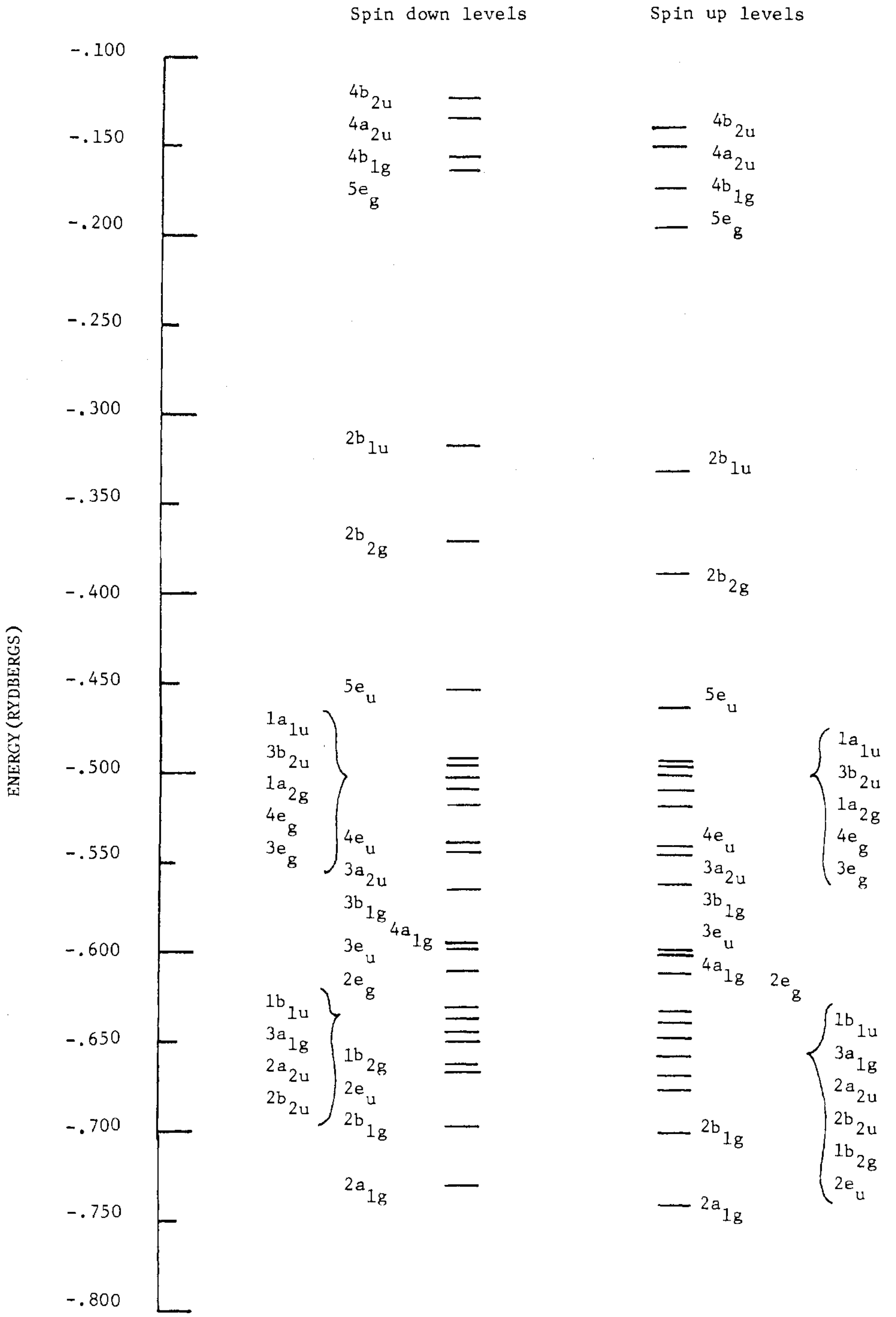

Figure 1. Upper valence region of the system, $Tc_2Cl_8^{3-}$. The highest occupied level is the $2b_{1u}\uparrow$ level.

structure established,[10] it was suggested[11] that this electron might occupy a nonbonding orbital of σ character concentrated in regions trans to the Tc–Tc bond, and this notion still appeared reasonable a few years later.[12]

In 1974 a detailed study[13] of the magnetic properties of the ion demonstrated that it has $\mu_{\text{eff}} = 1.78 \pm 0.03\ \mu_B$ from 80 to 300 K and that the g values are $g_{\parallel} = 1.912$ and $g_{\perp} = 2.096$. It was then pointed out[14] that g values with these relative magnitudes are not easily reconciled with such an orbital assignment but that, if the odd electron occupies a δ^* orbital, $g_{\perp} > g_{\parallel}$ might reasonably be expected. It was suggested, therefore that a δ^* assignment of the odd electron is preferable to that proposed earlier.

Some months after this revision was submitted, there appeared a brief report of a molecular orbital calculation[25] in the CNDO approximation leading to this same orbital assignment for the odd electron. However, since the CNDO approximation is a fairly drastic one, it remained questionable, at least in our minds, whether the conclusion could be accepted with full confidence. It was therefore considered worthwhile to carry out an SCF–Xα–SW calculation on the same system not only because the description thereby obtained of the ground-state electronic structure should be inherently more reliable but also because such a calculation can readily be extended to provide a detailed basis for discussing the optical spectrum. Comparison of theory and experiment with respect to the latter should afford a valuable check on the verisimilitude of the theoretical picture given by the calculation.

The ordering of the one-electron orbitals (Figure 1) for $Tc_2Cl_8^{3-}$ is qualitatively similar to that found earlier[18] for

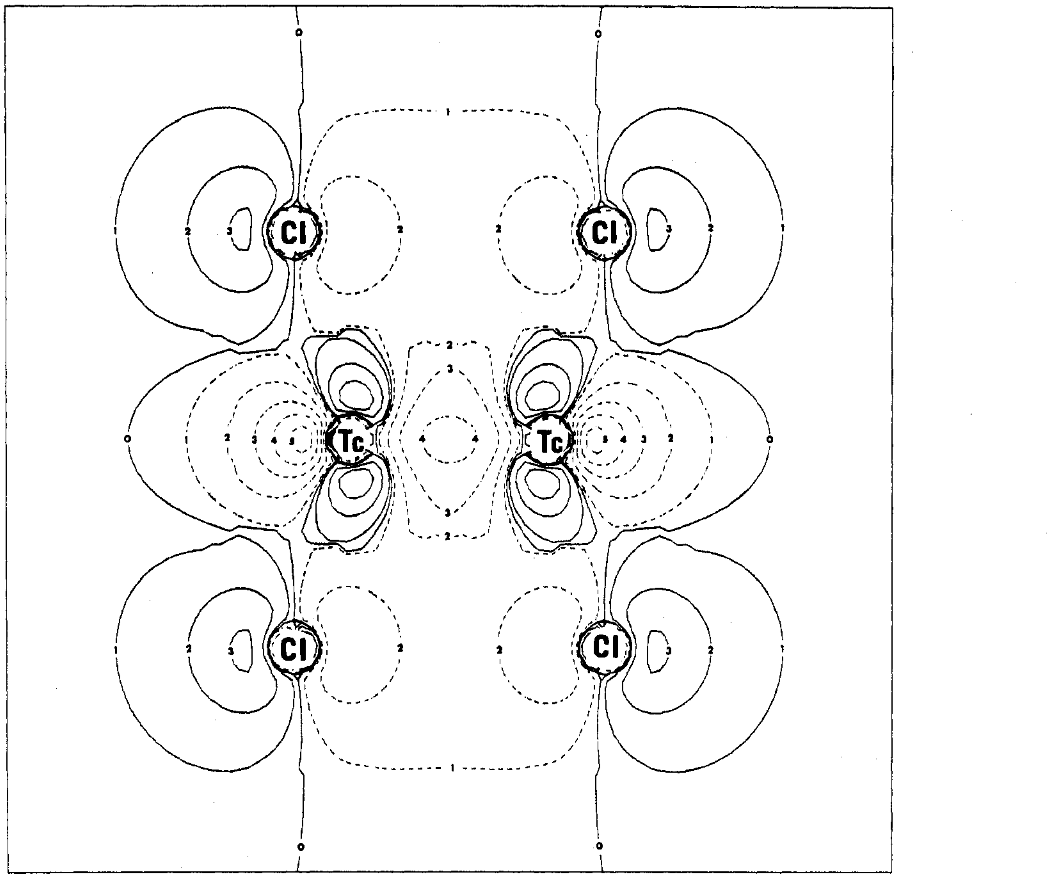

Figure 2. Contours of the $4a_{1g}$ level of $Tc_2Cl_8^{3-}$ for the converged one-electron eigenvalues obtained in the spin-restricted calculation. The metal–metal bond lies along the z axis. Contour values of 0, 1, 2, 3, 4, and 5 are equal to 0, 0.01, 0.04, 0.08, 0.12, and 0.16 $(\text{electrons/bohr}^3)^{1/2}$ and are the same for all plots. The total region plotted covers 18 × 18 bohrs^2.

$Mo_2Cl_8^{4-}$; the general electronic character and the metal–metal bonding in the two systems are similar, but there are some differences.

Both systems contain a set of low-lying valence levels of predominantly ligand 3s character (the $1a_{1g}$ to $1b_{2u}$ levels). These are followed by a set of levels of slightly higher energy (−0.744 to −0.609 Ry) which are responsible for most of the convalent metal–ligand interaction. These orbitals range in metal character from 10 to 71%. Orbitals of a_{1g}, a_{2u}, e_u, b_{1g}, e_g, and b_{2u} symmetries are appropriate for σ(M–Cl) bonding. The remaining levels are of the appropriate symmetry for π(M–Cl) interactions.

The participation of the na_{1g} (n = 2–4) levels in M–M σ bonding follows a considerably different pattern in the two complexes. In $Mo_2Cl_8^{4-}$ $2a_{1g}$ is largely (ca. 80%) Cl and $3a_{1g}$ is essentially all (ca. 90%) Cl in character and they play essentially no part in the Mo–Mo σ bond, which is due almost exclusively to the $4a_{1g}$ orbital. In $Tc_2Cl_8^{3-}$, however, the Tc–Tc σ bond receives important contributions from both the $4a_{1g}$ and the $2a_{1g}$ orbitals, which are shown in Figures 2 and 3, respectively. While $2a_{1g}$ is also Tc–Cl bonding to some extent, its most important role is as the major contributor to Tc–Tc σ bonding. The $3a_{1g}$ orbital again makes very little contribution to the metal–metal bonding.

As in $Mo_2Cl_8^{4-}$ the $5e_u$ level (Figure 4) is a major contributor to π(M–M) bonding, but again, as with the σ bonding, it shares this function with another e_u orbital, $2e_u$. In $Mo_2Cl_8^{4-}$ $5e_u$ has about 76% metal character and can be described fairly simply (and accurately) as "the" π(M–M) bonding orbital. The only other occupied π-type orbital having appreciable (~20%) metal d character in $Mo_2Cl_8^{4-}$ is $2e_u$, lying some 0.23 Ry lower. In $Tc_2Cl_8^{3-}$ the picture is not quite so simple; the $5e_u$ orbital has only about 52% metal character and $2e_u$ has about 46%. Nevertheless, as shown in Figure 4, the $5e_u$ orbital has excellent positive Tc–Tc overlap and is the principal source of π(M–M) bonding. It is, as Figure 4 shows quite clearly, antibonding with respect to Tc–Cl interaction.

Finally, we turn to the $\delta^*(2b_{1u})$ and $\delta(2b_{2g})$ orbitals. In each case these are of predominantly metal character although slightly less so in the $Tc_2Cl_8^{3-}$ case. In $Mo_2Cl_8^{4-}$ the δ orbital is the highest occupied orbital, the δ^* orbital is the lowest unoccupied orbital, and there are no nonbonding or antibonding orbitals in between; in fact, the next highest orbital ($4b_{1g}$) lies about 0.11 Ry higher than δ^*. The orbital pattern in this region is very much the same for $Tc_2Cl_8^{3-}$, with the distance from $\delta^*(2b_{1u})$ to the next lowest unoccupied orbital (~0.16 Ry) even greater. It turns out, therefore, that $\delta^*(2b_{1u})$ is occupied by the odd electron, as suggested by the EPR data and by Tondello's calculation.[25] The $\delta(2b_{2g})$ orbital is the highest doubly occupied orbital as in $Mo_2Cl_8^{4-}$ (and $Re_2Cl_8^{2-}$ as well).

Figure 5 shows the appearance of the $\delta(2b_{2g})$ level of $Tc_2Cl_8^{3-}$, while Figure 6 shows the $\delta^*(2b_{1u})$ orbital. It is quite clear that these orbitals do indeed have the bonding and antibonding character ascribed to them.

Ground State of $W_2Cl_8^{4-}$. The ordering of the energy levels here (Figure 7) may be compared to those of two other systems studied[17–19] by the Xα method: $Mo_2Cl_8^{4-}$ and $Re_2Cl_8^{2-}$. A table of the one-electron eigenvalues shows distinctly the presence of a quadruple bond made up principally of the $4a_{1g}$ (σ component), $5e_u$ (π component), and $2b_{2g}$ (δ component) levels. The contour plots of these levels are given in Figures 8–10. The $W_2Cl_8^{4-}$ system closely resembles its $Mo_2Cl_8^{4-}$ congener in that the $2a_{1g}$ level makes a relatively minor contribution to σ(M–M) bonding, as can be seen in Figure 11. The charge distribution between ligand and metal for the

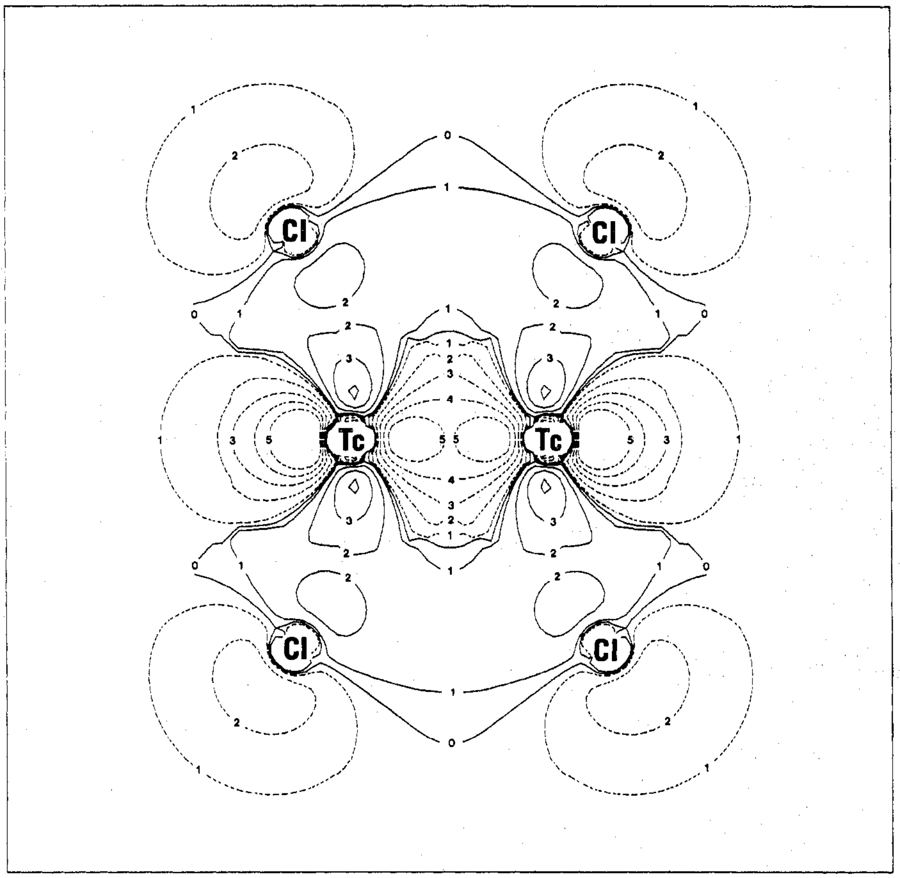

Figure 3. Contours of the $2a_{1g}$ level of $Tc_2Cl_8^{3-}$, plotted as for Figure 2.

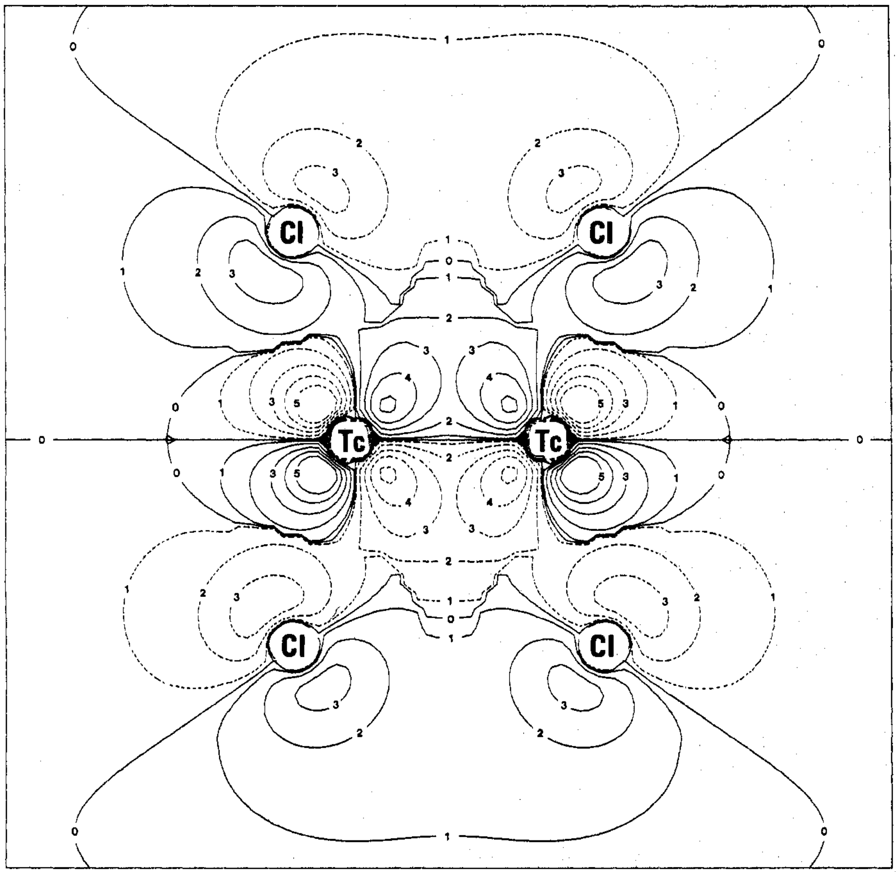

Figure 4. Contours of the $5e_u$ level of $Tc_2Cl_8^{3-}$ in the *yz* plane.

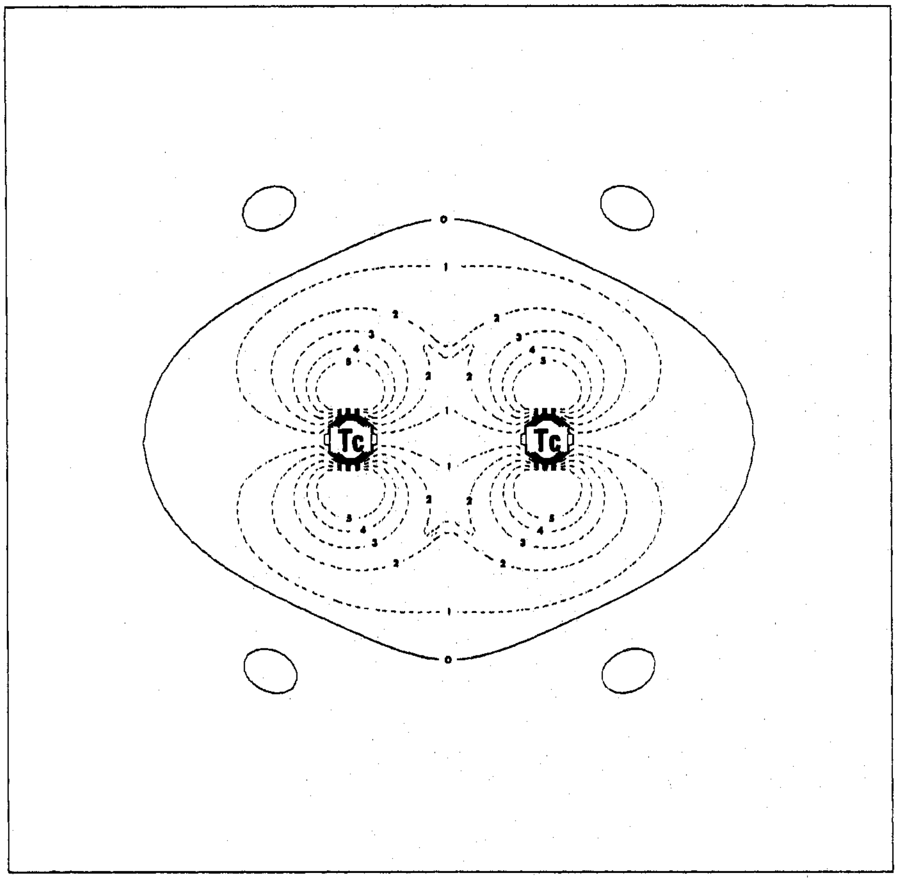

Figure 5. Contours of the $2b_{2g}$ level in $Tc_2Cl_8^{3-}$. These contours lie in a plane midway between the *xz* and *yz* planes, where the orbital wave function has its greatest negative amplitudes.

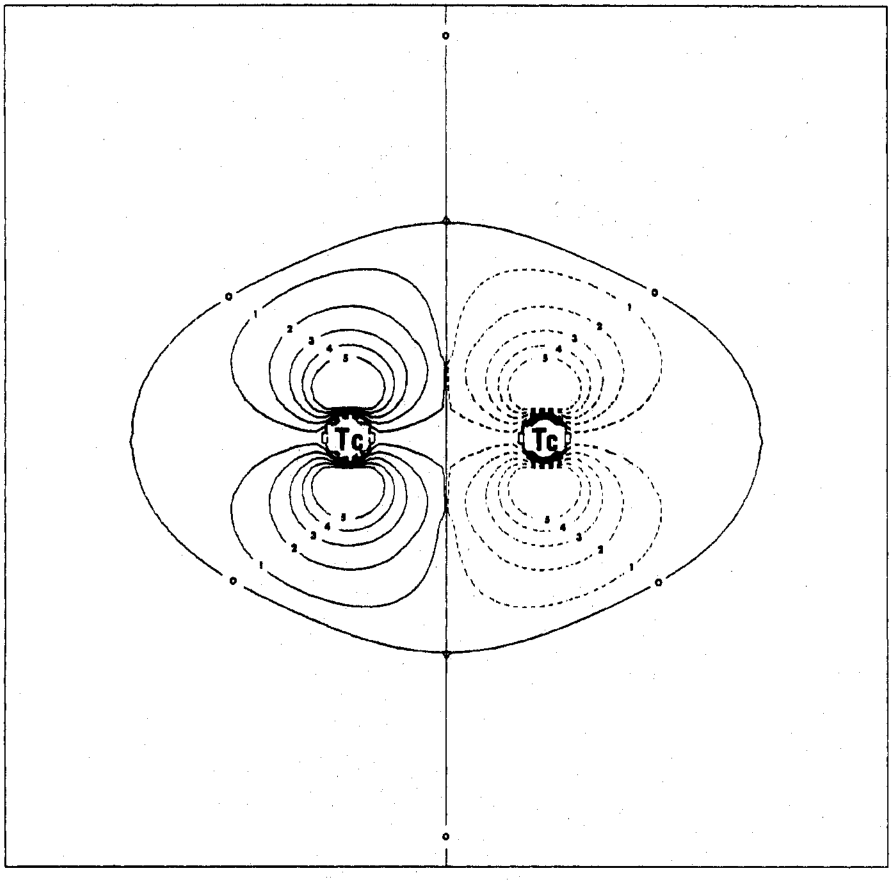

Figure 6. Plot of the $2b_{1u}$ level of $Tc_2Cl_8^{3-}$ shown in the same plane as for the $2b_{2g}$ level.

Table III. Ground-State Valence Energy Levels (Rydbergs) and Charge Distribution of $Tc_2Cl_8^{3-}$ for the Spin-Unrestricted Case[a]

Level	Energy	% 2 Tc	% 8 Cl	% OS	% IS
$5a_{2u}\downarrow$	−0.010	2.2	3.9	81.0	12.9
$5a_{2u}\uparrow$	−0.012	1.9	4.1	80.3	13.7
$6e_u\downarrow$	−0.017	0.1	5.5	73.3	21.1
$6e_u\uparrow$	−0.018	0.1	5.6	72.9	21.4
$5a_{1g}\downarrow$	−0.064	1.0	5.7	61.2	32.1
$5a_{1g}\uparrow$	−0.066	1.0	5.8	60.8	32.4
$4b_{2u}\downarrow$	−0.123	60.9	28.5	5.5	5.1
$4a_{2u}\downarrow$	−0.133	71.2	8.7	1.4	18.7
$4b_{2u}\uparrow$	−0.137	59.4	30.0	5.5	5.1
$4a_{2u}\uparrow$	−0.150	72.0	9.2	1.2	17.6
$4b_{1g}\downarrow$	−0.159	55.8	4.1	5.6	7.4
$5e_g\downarrow$	−0.170	82.6	9.5	0.2	7.8
$4b_{1g}\uparrow$	−0.173	54.4	32.7	5.4	7.4
$5e_g\uparrow$	−0.190	81.6	10.2	0.2	8.0
$2b_{1u}\downarrow$	−0.315	79.8	10.9	0.9	8.3
$2b_{1u}\uparrow$	−0.334	78.7	12.2	0.9	8.2
$2b_{2g}\downarrow$	−0.370	72.7	14.9	1.0	11.4
$2b_{2g}\uparrow$	−0.387	70.6	16.3	1.0	12.0
$5e_u\downarrow$	−0.454	47.3	39.9	1.5	11.3
$5e_u\uparrow$	−0.464	42.4	44.6	1.7	11.4
$1a_{1u}\downarrow$	−0.484	0	80.3	10.5	9.4
$1a_{1u}\uparrow$	−0.484	0	80.0	10.6	9.4
$3b_{2u}\downarrow$	−0.492	0	89.4	0.4	10.2
$3b_{2u}\uparrow$	−0.493	0	89.4	0.4	10.2
$1a_{2g}\downarrow$	−0.498	0	78.4	10.4	11.2
$1a_{2g}\uparrow$	−0.499	0	78.4	10.4	11.2
$4e_g\downarrow$	−0.508	1.1	87.3	4.0	7.5
$4e_g\uparrow$	−0.509	1.1	87.3	4.0	7.6
$3e_g\downarrow$	−0.518	2.7	84.6	0.3	12.5
$3e_g\uparrow$	−0.520	2.9	84.3	0.3	12.5
$4e_u\downarrow$	−0.536	7.5	78.8	2.9	10.8
$4e_u\uparrow$	−0.539	8.2	77.9	2.9	11.0
$3a_{2u}\downarrow$	−0.545	3.7	79.9	2.3	14.1
$3a_{2u}\uparrow$	−0.546	3.9	79.6	2.3	14.2
$3b_{1g}\downarrow$	−0.564	1.0	82.5	0.3	16.2
$3b_{1g}\uparrow$	−0.565	0.9	82.5	0.2	16.3
$4a_{1g}\downarrow$	−0.595	35.2	53.5	1.3	10.0
$3e_u\downarrow$	−0.597	3.2	79.9	2.3	14.5
$3e_u\uparrow$	−0.599	3.3	79.9	2.3	14.5
$4a_{1g}\uparrow$	−0.601	25.3	60.6	1.4	12.7
$2e_g\downarrow$	−0.609	10.1	77.3	0.3	12.4
$2e_g\uparrow$	−0.612	10.8	76.7	0.3	12.2
$1b_{1u}\downarrow$	−0.631	11.5	71.0	1.6	15.8
$1b_{1u}\uparrow$	−0.635	12.9	69.7	1.6	15.8
$3a_{1g}\downarrow$	−0.636	22.5	62.7	1.5	13.3
$3a_{1g}\uparrow$	−0.641	24.6	61.7	1.5	12.2
$2a_{2u}\downarrow$	−0.645	12.9	78.1	2.6	6.3
$2a_{2u}\uparrow$	−0.648	13.4	77.7	2.6	6.2
$2b_{2u}\downarrow$	−0.652	32.3	65.1	3.3	0.7
$2b_{2u}\uparrow$	−0.660	33.9	63.7	3.2	0.7
$1b_{2g}\downarrow$	−0.665	15.5	63.7	1.1	19.6
$2e_u\downarrow$	−0.667	42.2	45.0	0.9	11.9
$1b_{2g}\uparrow$	−0.669	17.3	62.1	1.1	19.5
$2e_u\uparrow$	−0.677	38.9	48.9	1.0	12.2
$2b_{1g}\downarrow$	−0.693	34.0	61.3	2.0	2.7
$2b_{1g}\uparrow$	−0.701	35.6	59.9	2.0	2.5
$2a_{1g}\downarrow$	−0.729	64.2	35.7	0.1	0
$2a_{1g}\uparrow$	−0.744	71.0	28.9	0.1	0
$1b_{2u}\downarrow$	−1.436	2.0	95.3	1.0	1.8
$1b_{2u}\uparrow$	−1.437	2.1	95.2	1.0	1.7
$1e_g\downarrow$	−1.439	1.2	94.8	0.7	3.3
$1e_g\uparrow$	−1.440	1.2	94.8	0.7	3.3
$1b_{1g}\downarrow$	−1.451	2.3	94.1	0.6	3.2
$1e_u\downarrow$	−1.452	1.2	93.9	0.8	4.1
$1b_{1g}\uparrow$	−1.452	2.4	94.0	0.6	4.1
$1e_u\uparrow$	−1.453	1.3	93.9	0.7	4.1
$1a_{2u}\downarrow$	−1.463	1.9	93.6	0.7	3.8
$1a_{2u}\uparrow$	−1.464	1.9	93.6	0.7	3.8
$1a_{1g}\downarrow$	−1.479	2.2	92.2	0.5	5.0
$1a_{1g}\uparrow$	−1.480	2.2	92.2	0.5	5.0

[a] The highest occupied level is the $2b_{1u}\uparrow$ level. The unoccupied levels were generated using the potential output for the final converged iteration of the ground state. Values for the charge distribution are given as the percent of charge in each level divided among the metal atoms, ligand atoms, and outer-sphere (OS) and inner-sphere (IS) regions.

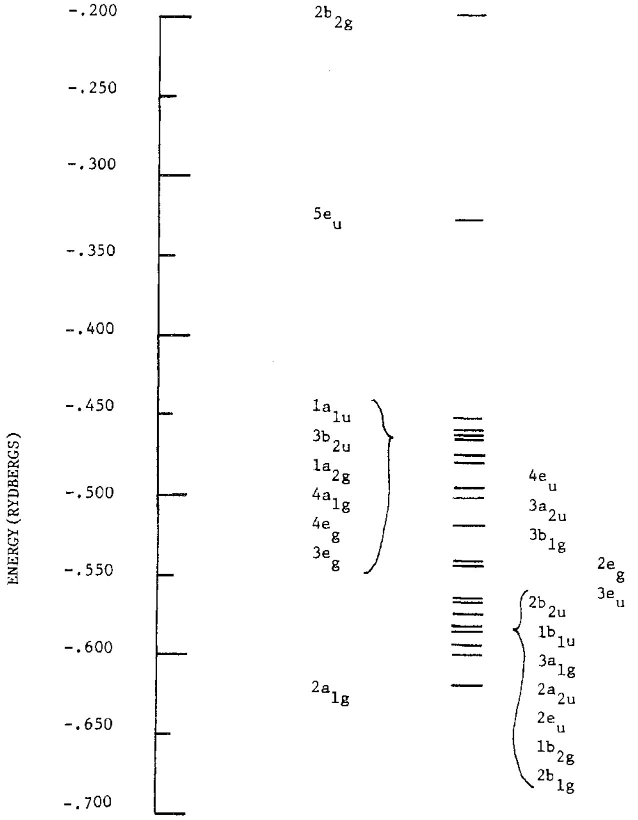

Figure 7. Upper level one-electron eigenvalues calculated for the $W_2Cl_8^{4-}$ ion.

δ bond in $W_2Cl_8^{4-}$ more closely resembles that in $Mo_2Cl_8^{4-}$ than that in $Re_2Cl_8^{2-}$. That is, it is an excellent approximation to consider the quadruple bond in $W_2Cl_8^{4-}$ as consisting predominantly of four metal 5d overlaps, whereas, in $Re_2Cl_8^{2-}$ as in $Tc_2Cl_8^{3-}$, the various contributions to the quadruple bonds are less simply described. This is an accord with the argument to be presented below that change in effective nuclear change has a pronounced effect on metal–ligand and metal–metal interactions.

The predominantly metal character of the $\delta(2b_{2g})$ level (and presumably $\delta^*(2b_{1u})$ level) is reflected in the low-lying orbitals responsible for metal–ligand π overlap. The $1b_{2g}$ and $1b_{1u}$ levels in $Re_2Cl_8^{2-}$ possess substantial metal character, presumably because of extensive mixing with the δ and δ^* orbitals ($2b_{2g}$ and $2b_{1u}$), respectively. The $1b_{2g}$ and $1b_{1u}$ levels of $W_2Cl_8^{4-}$, however, have very little metal character.

On the other hand, as for $Re_2Cl_8^{2-}$, the $3e_u$ and $4e_u$ levels are ligand nonbonding and do not interact with the $5e_u$ level. The $2e_u$ level responsible for σ(M–Cl) bonding does show some metal character (16.5%), but this is greatly reduced when compared to that observed in $Re_2Cl_8^{2-}$ where the metal contribution is 43.7%.

The calculation on $W_2Cl_8^{4-}$ gives no indication that this ion should be incapable of existence or even particularly unstable on the basis of total energies or core repulsion energies compared with the cases of $Mo_2Cl_8^{4-}$, $Re_2Cl_8^{2-}$, and $Tc_2Cl_8^{3-}$. The pattern of orbitals and their energies for $W_2Cl_8^{4-}$ seem to be just what one might reasonably have expected by extrapolation from the $Mo_2Cl_8^{4-}$, $Tc_2Cl_8^{3-}$, and $Re_2Cl_8^{2-}$ results and thus suggest that the stability of $W_2Cl_8^{4-}$ should not be *drastically* less than the stabilities of these other $M_2Cl_8^{n-}$ species. We were sufficiently encouraged by this result, which was obtained in late 1975, to launch new efforts to prepare $W_2Cl_8^{4-}$ or some comparable $W_2X_8^{4-}$ species containing W–W quadruple bonds. We were also encouraged, of course, by the discovery, at about the same time, that molecules with W–W

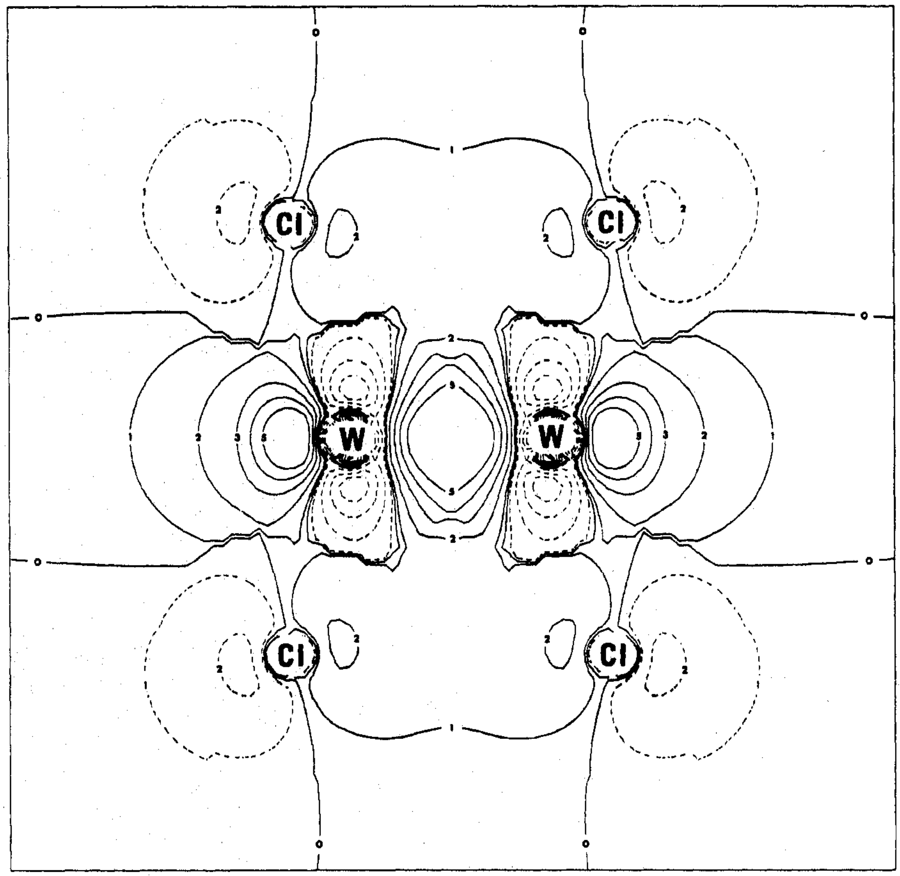

Figure 8. Contour map of the $4a_{1g}$ level of $W_2Cl_8^{4-}$.

Table IV. Ground-State Total Energies (Rydbergs), Virial Ratios, and Charge Distributions (Electrons)

	$Tc_2Cl_8^{3-}$		
	Spin restricted	Spin unrestricted	$W_2Cl_8^{4-}$
Total energy	−24 172.61	−24 171.91	−68 506.94
Kinetic energy	24 181.73	24 203.91	68 510.94
Potential energy	−48 354.34	−48 375.82	−137 017.9
$-2T/V$	1.000 187 9	1.000 660 9	1.000 028 6
Total charge in various regions			
2 Tc or W	83.687	83.656	145.624
8 Cl	133.657	133.676	134.524
Extramolecular	1.021	0.989	1.473 18
Inner sphere	6.633	6.678	6.377 08

Table V. Atomic Coordinates, α Parameters, and Sphere Radii for $W_2Cl_8^{4-}$ (Atomic Units)

	x	y	z	α	R
W(1)	0.0	0.0	2.0770	0.6993	2.5661
W(2)	0.0	0.0	−2.0770	0.6993	2.5661
Cl(1)	−4.4903	0.0	3.2802	0.72325	2.7045
Cl(2)	0.0	−4.4903	3.2802	0.72325	2.7045
Cl(3)	0.0	4.4903	3.2802	0.72325	2.7045
Cl(4)	4.4903	0.0	3.2802	0.72325	2.7045
Cl(5)	−4.4903	0.0	−3.2802	0.72325	2.7045
Cl(6)	0.0	−4.4903	−3.2802	0.72325	2.7045
Cl(7)	0.0	4.4903	−3.2802	0.72325	2.7045
Cl(8)	4.4903	0.0	−3.2802	0.72325	2.7045
Extramolecular	0.0	0.0	0.0	0.71046	7.8649

triple bonds[26,27] are as easily prepared and as stable as those with Mo–Mo triple bonds.[28]

We have not yet succeeded in isolating a compound containing the $W_2Cl_8^{4-}$ ion, but the compounds $Li_4W_2(CH_3)_8$·4(ether) and a substance containing mixed-ligand complexes with compositions averaging to $W_2(CH_3)_xCl_{8-x}$ (x = 4–6) have been prepared and the latter has been characterized structurally.[29] The W–W distance found is 2.26 Å, which is 0.06 Å longer than that assumed in the calculation. We have not considered it worthwhile to repeat the calculation, since the small increase in distance will have only a small quantitative effect and no qualitative effect upon the results for the ground-state electron structure. Both $Li_4W_2(CH_3)_8$ and $Li_4W_2(CH_3)_xCl_{8-x}$ are extremely heat and air sensitive, decomposing when the reaction temperature is allowed to rise above −20 °C. This feature is in accord with the orbital scheme as calculated for the $W_2Cl_8^{4-}$ system. The $2b_{2g}$ level is of extremely high energy compared to the $2b_{2g}$ levels in the quadruply bonded systems, $Mo_2Cl_8^{4-}$ and $Re_2Cl_8^{2-}$ (i.e., less stable by 0.112 and 0.289 Ry, respectively). Similarly, the $5e_u$ orbital is also less stable in $W_2Cl_8^{4-}$ by 0.081 Ry compared to the $5e_u$ level in $Mo_2Cl_8^{4-}$ and by 0.223 Ry compared to the $Re_2Cl_8^{2-}$ system. It is reasonable to postulate that the destabilization of the δ orbital in $W_2Cl_8^{4-}$ should readily lead to oxidation or oxidative addition reactions involving the quadruple bond. This would account for the large number of triply bonded tungsten complexes which have been isolated to date and the correspondingly small number of W–W quadruply bonded systems. It has already been established that molybdenum(II) systems of stoichiometry $Cs_3Mo_2Cl_7$ are

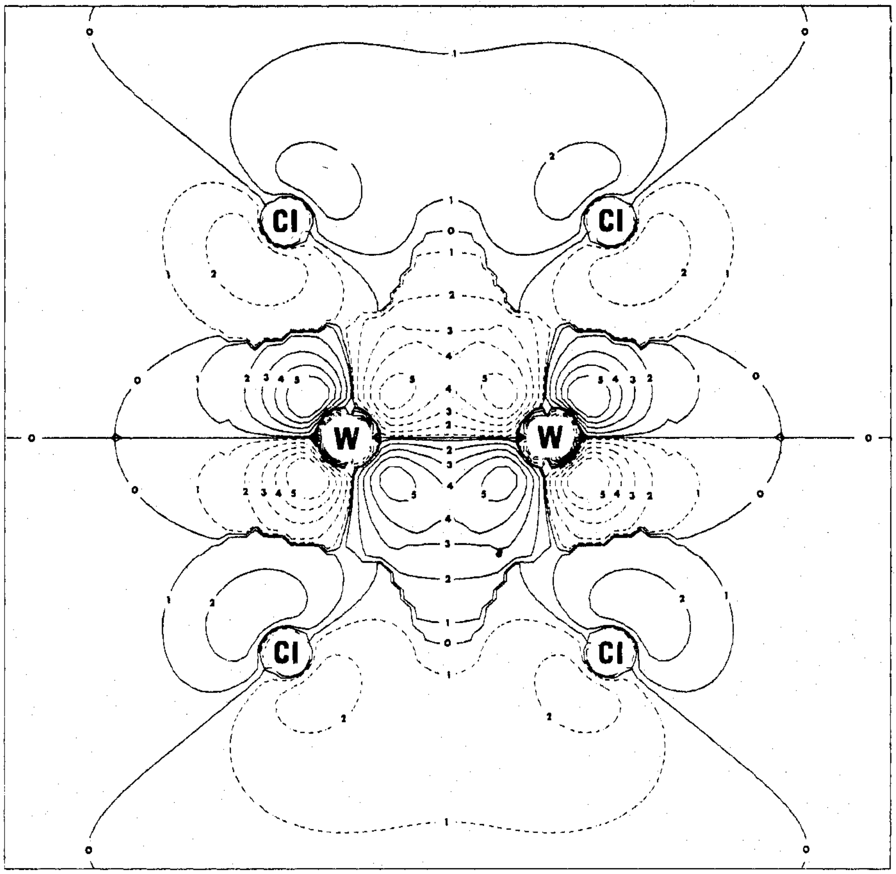

Figure 9. Contours of the $5e_u$ level for the $W_2Cl_8^{4-}$ system.

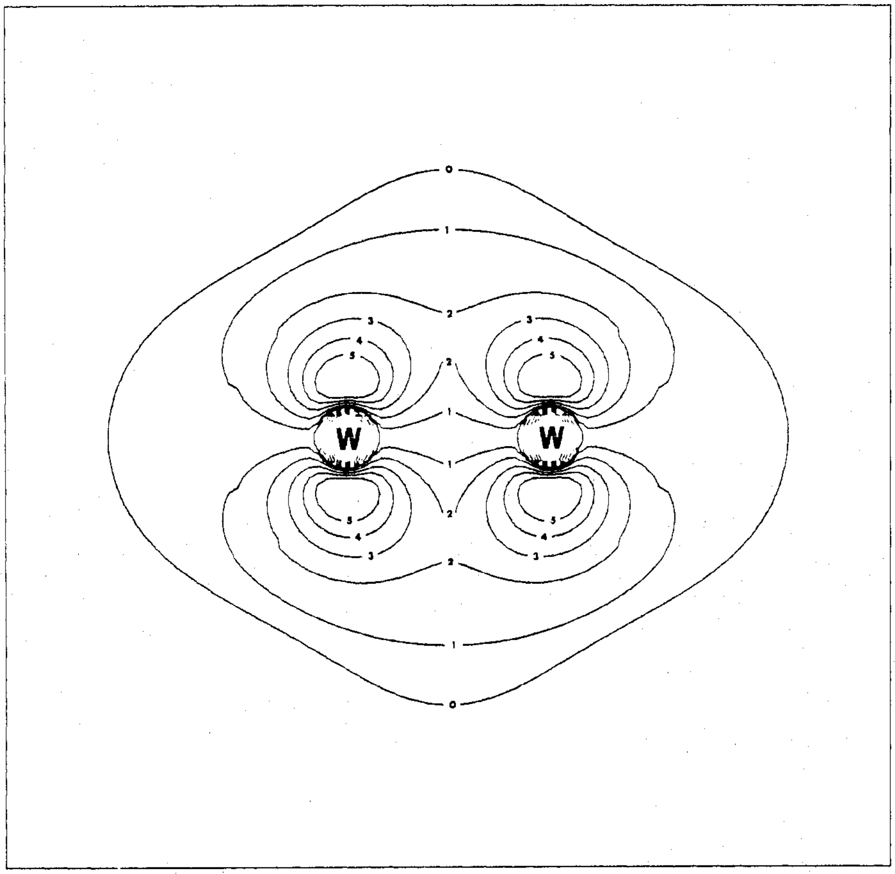

Figure 10. Plot of the $2b_{2g}$ orbital of $W_2Cl_8^{4-}$. Contour values are the same as those for the $2b_{2g}$ level of $Tc_2Cl_8^{3-}$.

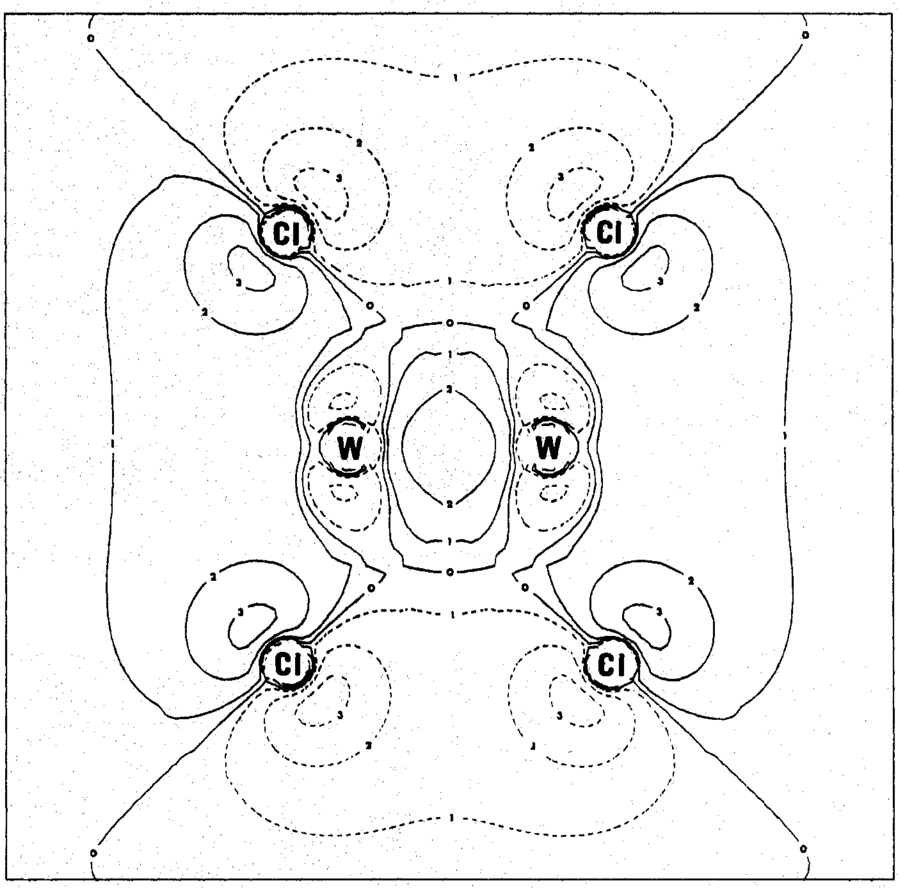

Figure 11. Plot of the $2a_{1g}$ orbital of $W_2Cl_8^{4-}$. Contour levels are as in Figure 2.

Table VI. Ground-State Valence Level One-Electron Eigenvalues (Rydbergs) for $W_2Cl_8^{4-}$

		Distribution of charge			
Level	Energy	% 2 W	% 8 Cl	% IS	% OS
$2b_{2g}$	−0.198	74.7	8.0	15.7	1.6
$5e_u$	−0.327	69.5	17.3	12.2	1.1
$1a_{1u}$	−0.453	0.0	93.1	10.7	11.7
$3b_{2u}$	−0.462	0.1	89.1	10.3	0.5
$1a_{2g}$	−0.464	0.0	88.3	10.4	1.4
$4a_{1g}$	−0.466	82.6	16.5	0	0.8
$4e_g$	−0.475	1.2	87.3	7.2	4.2
$3e_g$	−0.480	2.3	86.2	9.4	2.2
$4e_u$	−0.496	4.4	82.5	9.8	3.2
$3a_{2u}$	−0.501	2.0	82.0	13.4	2.6
$3b_{1g}$	−0.519	9.5	83.5	13.5	2.1
$2e_g$	−0.542	5.5	81.1	10.3	3.0
$3e_u$	−0.544	2.2	80.7	14.6	2.4
$2b_{2u}$	−0.568	20.0	75.1	0.5	4.3
$1b_{1u}$	−0.569	5.2	76.3	16.5	2.0
$3a_{1g}$	−0.574	8.4	73.1	16.2	2.3
$2a_{2u}$	−0.579	9.8	79.8	7.5	2.9
$2e_u$	−0.581	16.5	67.4	14.4	1.7
$1b_{2g}$	−0.593	7.1	71.0	20.0	2.0
$2b_{1g}$	−0.600	21.9	71.0	3.0	4.2
$2a_{1g}$	−0.618	27.6	63.6	5.4	3.5
$1b_{2u}$	−1.352	1.6	95.3	2.0	1.1
$1e_g$	−1.353	1.1	94.8	3.0	1.1
$1b_{1g}$	−1.363	1.8	94.3	2.9	1.0
$1e_u$	−1.363	1.2	93.9	4.0	0.8
$1a_{2u}$	−1.372	6.1	93.7	4.0	8.1
$1a_{1g}$	−1.384	1.7	92.6	4.9	0.9

capable of undergoing dinuclear oxidative addition reactions to give the molybdenum(III) product, $Cs_3Mo_2Cl_8H$.[30]

We are currently carrying out SCF–Xα–SW calculations on the series $Cr_2(CH_3)_8^{4-}$, $Mo_2(CH_3)_8^{4-}$, and $W_2(CH_3)_8^{4-}$, since optical spectra of all of these are available,[29,31] and the results of that study should satisfactorily characterize the W–W quadruple bond, in the octamethyl system, and allow an informative comparison with the Mo–Mo and Cr–Cr quadruple bonds.

Comparisons between the Four $M_2Cl_8^{n-}$ Calculations. When the results now available for the four systems, $Tc_2Cl_8^{3-}$, $Mo_2Cl_8^{4-}$, $W_2Cl_8^{4-}$, and $Re_2Cl_8^{2-}$, are all compared, several points of general interest emerge.

(1) If we discount the $1a_{1u}$ orbital, which is a nonbonding orbital of purely ligand character, the pattern in descending order of energy $\delta^*(2b_{1u}) > \delta(2b_{2g}) > \pi(5e_u)$, in the center of the orbital diagram, with a considerable gap between δ^* and the next lowest antibonding orbital, is a consistent feature.

(2) As might be expected, the overall charge on the $M_2X_8^{n-}$ ion correlates qualitatively with the variation in orbital energies from one species to another. Thus, the entire pattern of MO's lies highest for the 4− ions, lower for $Tc_3Cl_8^{3-}$, and lowest for $Re_2Cl_8^{2-}$. The energies of the $5e_u$ levels, for example, are −0.327 (W), −0.408 (Mo), −0.458 (Tc), and −0.550 Ry (Re).

(3) The extent of mixing of metal and ligand character in the MO's generally increases as the formal oxidation number of the metal increases. Thus in the $M_2X_8^{4-}$ ions the M–M bonding comes closest to the pure metal d orbital approximation[2] first used to give a qualitative MO picture of the quadruple bond. The mixing in of ligand character increases substantially in the Tc and Re species, thus making the original simple idea a less accurate approximation. To take again the $5e_u$ orbitals for illustration, they have 76% metal character in the $Mo_2Cl_8^{4-}$ species, only 52% for $Tc_2Cl_8^{3-}$, and only 47% for $Re_2Cl_8^{2-}$. The approximate numbers just given involve a small rescaling of the numbers given in our tables and for the Re system in order to allow direct comparison with numbers previously given for the Mo compound, since the percents given for the latter were calculated in such a way that

the charges included within atomic spheres were scaled to total 100%.

Optical Spectrum of $Tc_2Cl_8^{3-}$. The optical spectrum of this ion has not been reported in detail as yet, but such a study is in progress.[16] It has been found that there is a broad band with a decadic molar extinction coefficient of about 600 centered at about 6800 cm^{-1}. Moreover, this band exhibits vibrational structure even at room temperature and data at ca. 15 K indicate that there are perhaps two overlapping progressions, one with a spacing of 330 ± 30 cm^{-1}. The intensity of this band is essentially independent of temperature. All of this is very reminiscent of the characteristics of the band at ca. 14 000 cm^{-1} in the $Re_2Cl_8^{2-}$ spectrum[32] and it is our tentative suggestion, on the experimental evidence alone, that this band may be the $\delta \rightarrow \delta^*$ transition, as is definitely the case[33,34] with the 14 000-cm^{-1} band in $Re_2Cl_8^{2-}$.

The calculation on $Tc_2Cl_8^{3-}$ has been extended to afford predictions of the energies of the electronic transitions expected in the near-IR, visible, and near-UV regions. We shall not enter into a full and detailed discussion of these results here, pending the completion of additional experimental work, but we can report that the predicted position of the $\delta \rightarrow \delta^*$ transition, ca. 6000 cm^{-1}, is in excellent agreement with the energy of the band mentioned above. The vibrational progressions constituting this band actually begin at ca. 5900 cm^{-1}. In addition, we predict the $2b_{1u} \rightarrow 5e_g$ ($^2E_g \leftarrow {}^2B_{1u}$) transition to be at ca. 15 000 cm^{-1}, which matches rather well the position of the band ($\epsilon \sim 170$) already known[12] to occur at ca. 16 000 cm^{-1}. It is to be noted that for $Tc_2Cl_8^{3-}$, the $\delta \rightarrow \delta^*$ transition is a doublet–doublet transition and can therefore be computed more straightforwardly than in the cases of $Mo_2Cl_8^{4-}$ and $Re_2Cl_8^{2-}$, where both singlet–singlet and singlet–triplet components need to be considered. In any event, our calculation, assuming the assignment suggested is correct, comes much closer to the observed value than did the calculations in either of the other two cases.

Acknowledgment. We thank the National Science Foundation for financial support and Professor J. G. Norman, Jr., of the University of Washington for advice. We are very grateful to Mr. George G. Stanley for his extensive help in providing all of the contour plots.

Registry No. $Tc_2Cl_8^{3-}$, 53260-19-8; $W_2Cl_8^{4-}$, 62929-94-6.

Supplementary Material Available: Tables S-I (core levels of $Tc_2Cl_8^{3-}$, spin restricted), S-II (core levels of $Tc_2Cl_8^{3-}$, spin unrestricted), and S-III (core levels of $W_2Cl_8^{4-}$) (3 pages). Ordering information is given on any current masthead page.

References and Notes

(1) F. A. Cotton, N. F. Curtis, C. B. Harris, B. F. G. Johnson, S. J. Lippard, J. T. Mague, W. R. Robinson, and J. S. Wood, *Science*, **145**, 1305 (1964).
(2) F. A. Cotton, *Inorg. Chem.*, **4**, 334 (1965).
(3) F. A. Cotton, *Chem. Soc. Rev.*, **4**, 27 (1975).
(4) J. C. Slater, *Adv. Quantum Chem.*, **6**, 1 (1972).
(5) J. C. Slater and K. H. Johnson, *Phys. Rev. B*, **5**, 844 (1972).
(6) K. H. Johnson, J. G. Norman, Jr., and J. W. D. Connolly, "Computational Methods for Large Molecules and Localized States in Solids", Plenum Press, New York, N.Y., 1972.
(7) K. H. Johnson, *Annu. Rev. Phys. Chem.*, **26**, 39 (1975).
(8) K. H. Johnson, *Adv. Quantum Chem.*, **7**, 143 (1973).
(9) J. D. Eakens, D. G. Humphreys, and E. D. Mellish, *J. Chem. Soc.*, 6012 (1963).
(10) F. A. Cotton and W. K. Bratton, *J. Am. Chem. Soc.*, **87**, 921 (1965).
(11) F. A. Cotton, *Rev. Pure Appl. Chem.*, **17**, 25 (1967).
(12) W. K. Bratton and F. A. Cotton, *Inorg. Chem.*, **9**, 789 (1970).
(13) F. A. Cotton and E. Pedersen, *Inorg. Chem.*, **14**, 383 (1975).
(14) F. A. Cotton and E. Pedersen, *J. Am. Chem. Soc.*, **97**, 303 (1975).
(15) F. A. Cotton and L. W. Shive, *Inorg. Chem.*, **14**, 2032 (1975).
(16) Optical and vibrational spectra measured here and at Iowa State University by L. D. Gage, P. E. Fanwick, and Professor D. S. Martin.
(17) J. G. Norman, Jr., and H. J. Kolari, *J. Chem. Soc., Chem. Commun.*, 303 (1974).
(18) J. G. Norman, Jr., and H. J. Kolari, *J. Am. Chem. Soc.*, **97**, 33 (1975).
(19) A. P. Mortola, J. W. Moskowitz, and N. Rosch, *Int. J. Quantum Chem., Symp.*, **No. 8**, 161 (1974).
(20) R. E. Watson, *Phys. Rev.*, **111**, 1108 (1958).
(21) K. Schwarz, *Phys. Rev. B*, **5**, 2466 (1972).
(22) J. G. Norman, Jr., *J. Chem. Phys.*, **61**, 4630 (1974).
(23) K. Schwarz, *Theor. Chim. Acta*, **34**, 225 (1974).
(24) E. A. Kmetko, *Phys. Rev. A*, **1**, 37 (1970).
(25) M. Biagini Cingi and E. Tondello, *Inorg. Chim. Acta*, **11**, L3 (1974).
(26) M. H. Chisholm, F. A. Cotton, M. Extine, M. Millar, and B. R. Stults, *Inorg. Chem.*, **15**, 2244 (1976).
(27) M. H. Chisholm, F. A. Cotton, M. Extine, and B. R. Stults, *Inorg. Chem.*, **15**, 2252 (1976).
(28) M. H. Chisholm, F. A. Cotton, B. A. Frenz, W. W. Reichert, L. W. Shive, and B. R. Stults, *J. Am. Chem. Soc.*, **98**, 4469 (1976).
(29) D. L. Collins, F. A. Cotton, S. Koch, M. Millar, and C. A. Murillo, *J. Am. Chem. Soc.*, **99**, 1259 (1977).
(30) F. A. Cotton and B. J. Kalbacher, *Inorg. Chem.*, **15**, 522 (1976).
(31) A. P. Sattelberger and J. P. Fackler, *J. Am. Chem. Soc.*, **99**, 1258 (1977).
(32) C. D. Cowman and H. B. Gray, *J. Am. Chem. Soc.*, **95**, 8177 (1973).
(33) A. P. Mortola, J. W. Moskowitz, N. Rosch, C. D. Cowman, and H. B. Gray, *Chem. Phys. Lett.*, **32**, 283 (1975).
(34) F. A. Cotton, B. A. Frenz, B. R. Stults, and T. R. Webb, *J. Am. Chem. Soc.*, **98**, 2868 (1976).